scientific reports

Check for updates

OPEN

Glaucocalyxin A alleviates ulcerative colitis by inhibiting PI3K/AKT/mTOR signaling

Tongtong Zhou[1,4], Yujing Ye[1,4], Weijie Chen[1,2], Yanyan Wang[1], Lulu Ding[1], Yicun Liu[3], Leilei Luo[3], Lixian Wei[3], Jian Chen[3] & Zhaolian Bian[3]✉

Isodon japonicus **(Burm.f.) Hara var. glaucocalyx (Maxim.) Hara is a herbaceous perennial plant. Historically, it has often been used to treat dysentery and other diseases, indicating its potential efficacy in the treatment of inflammatory conditions affecting the intestines. Glaucocalyxin A (GLA) is a diterpenoid isolated from *I. japonicus*; recent studies have revealed that it exhibits a range of biological activities, including neuroprotective, anticancer, anti-inflammatory, hepatoprotective, and anti-fibrotic effects. However, previous studies have not specifically explored the mechanism whereby GLA alleviates ulcerative colitis (UC). Therefore, in the present study, we generated a DSS-induced UC mouse model and lipopolysaccharide-induced RAW264.7 inflammation model and performed network pharmacology analysis and peripheral blood analysis of patients with acute UC to investigate the mechanisms underlying the positive effects of GLA on UC. This study demonstrated the anti-inflammatory effects of GLA in a mouse model of DSS-induced UC. Network pharmacology analysis revealed that AKT is a common target of GLA and inflammatory bowel disease (IBD). The changes in LPS-induced RAW264.7 cell inflammation further verified that GLA reduced the expression of inflammatory cytokines by inhibiting PI3K/AKT/mTOR signaling. Finally, in vitro magnetic bead sorting experiments showed that GLA could be used in the treatment of UC patients.**

Keywords Inflammatory bowel disease, Macrophage, Network pharmacology, Glaucocalyxin A, $CD14^+$, PI3K/AKT/mTOR

Ulcerative colitis (UC) is a serious gastrointestinal disorder that presents with symptoms such as persistent diarrhea, blood and mucus in the stool, abdominal pain, fatigue, and weight loss[1]. The prevalence of this chronic condition is steadily increasing each year and affects millions of people worldwide[2]. The mechanism of inflammatory bowel disease (IBD) is not well understood and can be attributed to the interplay among prenatal heredity, abnormal immune systems, and environmental factors[3]. Despite significant advancements in biological therapies for IBD over the past few decades, these therapies may be ineffective or cause serious complications[4]. Prolonged physical discomfort and poor treatment outcomes place significant physiological stress on patients and negatively affect their mental health. Therefore, exploring new treatment approaches to alleviate symptoms and reduce the need for surgical intervention is of great importance.

Macrophages are crucial for maintaining intestinal immune balance and can inhibit excessive inflammatory responses through multiple mechanisms[5,6], promote inflammation, and suppress inflammatory responses. In IBD, we found that macrophage overactivation greatly increases the release of inflammatory cytokines, including TNF-α and IL-6[7]. These pro-inflammatory cytokines attract and activate neutrophils and lymphocytes, thereby further exacerbating intestinal inflammatory yresponses and leading to a series of pathophysiological processes[8].

AKT is a crucial component of the PI3K/AKT signaling pathway. In rheumatoid arthritis (RA), excessive activation of AKT leads to the sustained production of inflammatory mediators and the destruction of joint tissues. Moreover, aberrant AKT activation is associated with the exacerbation of intestinal inflammation and tissue damage[9]. Therefore, modulating AKT signaling may represent a novel strategy for the treatment of inflammation-related diseases. Several studies have demonstrated the ability of the AKT pathway to regulate inflammatory responses. AKT often plays a key role in various physiological and pathological conditions[9].

[1]Medical School, Nantong University, Nantong 226001, Jiangsu Province, China. [2]Department of Gastroenterology, Shanghai Tenth People's Hospital, School of Medicine, Tongji University, Shanghai 200092, China. [3]Department of Gastroenterology and Hepatology, Nantong Third People's Hospital, Affiliated Nantong Hospital 3 of Nantong University, No. 60 Middle Qingnian Road, Nantong 226006, Jiangsu Province, China. [4]Tongtong Zhou and Yujing Ye equally contributed to this work. ✉email: bianzhaolian1998@163.com

Activation of AKT exacerbates macrophage dysfunction and inflammation, which can increase the release of inflammatory mediators[10]. Further studies have found that AKT directly phosphorylates the inhibitory protein PRAS40 of mTOR complex 1 (mTORC1), relieving its suppression of mTOR, thereby activating downstream pro-inflammatory pathways[11]. Studies have found that the activation of p-mTOR promotes the secretion of pro-inflammatory cytokines (such as IL-6 and TNF-α), thereby exacerbating the inflammatory response and tissue damage[9,12]. Based on this mechanism, recent studies have shown that many monomeric compounds from traditional Chinese medicine may effectively alleviate the pathological progression of UC by targeting and inhibiting the PI3K/AKT/mTOR signaling pathway[13–15].

Isodon japonicus (Burm.f.) Hara var. glaucocalyx (Maxim.) Hara has been widely used in traditional medicine for the treatment of diarrhea[16]. This plant contains many active ingredients, including diterpenoids, which exert anti-inflammatory effects. During the last decade, Glaucocalyxin A (GLA) has been shown to have anti-inflammatory, antitumor, antioxidant, and antifibrosis activity[17–19]. Studies have revealed that GLA can suppress PI3K/Akt signaling, alleviating the progression of bladder cancer[18]. Additionally, GLA alleviates the inflammatory response in osteoarthritic chondrocytes induced by IL-1β[20]. Therefore, we speculate that GLA may alleviate UC.

Materials and methods

Chemical reagents

GLA (99.56% purity) was purchased from TargetMol (CAS 79498-31-0; Boston, MA, USA) (Fig. 4A). Dimethyl sulfoxide (DMSO) and lipopolysaccharide (LPS) were purchased from Sigma-Aldrich (Munich, Germany). DSS (36–50 kDa) was acquired from MP Biomedicals (Irvine, CA, USA). RNAiso Plus, Reverse Transcription Kit, and SYBR Green Master Mix were purchased from Takara Bio, Inc (Beijing, China). All antibodies used for western blotting were obtained from CST (Danvers, MA, USA).

Animals and acute colitis induction

Male C57BL/6J wild-type mice aged six to eight weeks were obtained from the Laboratory Animal Center affiliated with the Institute of Pharmaceutical Sciences at the Shanghai Academy of Sciences, China. The mice were housed in Specific Pathogen-Free (SPF) conditions at Nantong University's Laboratory Animal Center, maintained under a 12-h light/dark cycle at room temperature, and provided ad libitum access to sterile food and water. Before the experiments began, the mice underwent a one-week acclimation period. All protocols and procedures conformed to the guidelines of the Nantong University Committee for Care and Use of Laboratory Animals and were approved by the Animal Experiments Ethics Committee of Nantong University. Acute UC was induced by administering 3% DSS in the drinking water for one week. Forty mice were randomly assigned to the negative control, DSS, and GLA treatment groups (20 and 40 mg/kg) (Fig. 1A). Except for the negative control group, mice in all other groups were allowed free access to 3% DSS in their drinking water for seven consecutive days. Throughout the experimental period, the same researcher administered intraperitoneal injections of GLA at doses of 20 and 40 mg/kg in the treatment groups each day. Meanwhile, the DSS group received intraperitoneal injections of the solvent used to dissolve GLA. The fecal condition (color and consistency) and body weight of each mouse in each group were recorded at the same time every day. A fecal occult blood test kit was used daily to determine the occult blood score of fresh feces from each mouse in each group. On the 8th day, each group of mice was euthanized by exposure to 40% carbon dioxide gas in a well-ventilated room. Animals were placed into a transparent euthanasia chamber equipped with a flow meter and not pre-filled with carbon dioxide. Carbon dioxide was introduced into the chamber at a rate of 30% of the chamber's volume per minute for 10 min. The animals were confirmed to be motionless, not breathing, and with dilated pupils. The carbon dioxide supply was then turned off, and the mice were observed for an additional 3 min to confirm death. To evaluate UC severity, we documented changes in body weight and daily feces characteristics and measured the full length of the colon for each group. Colon tissues from each group were collected for further analysis.

Histopathology and scoring criteria

The colons were washed with phosphate-buffered saline. Using pipette tips and blades, the entire colon tissue was processed into a 'Swiss roll,' secured with insect pins, and then placed in 35% formaldehyde solution for 24 h for fixation. After embedding the tissue samples in paraffin, they were sliced into 4-μm-thick sections and stained with HE. Sections were observed using a fluorescence electron microscope (OLYMPUS TH4-200), and intestinal injury was scored. Inflammation severity was scored 0 for normal, 1 for mild, 2 for moderate, and 3 for severe. The injury depth was rated 0 for normal, 1 for mucosal involvement, 2 for submucosal involvement, and 3 for transmural damage. Crypt damage was scored as follows: 0 for normal, 1 for one-third affected, 2 for two-thirds affected, and 3 for superficial epithelium intact only. The affected area was scored from 0 to 4, with 0 for normal involvement and 4 for 76–100% involvement[21], and the scoring results were statistically analyzed using GraphPad Prism 9.5.0.

Immunohistochemistry

Paraffin sections were prepared as described above and then deparaffinized in water. Antigen retrieval was performed using a citrate buffer (pH 6.0) (G1201) for 10 min. The sections were placed in a 3% hydrogen peroxide solution to block endogenous peroxidase activity. The tissue sections were evenly covered with 5% BSA and blocked and then incubated with primary antibodies, namely, myeloperoxidase recombinant antibodies (Rabbit mAb) at a 1:1000 dilution (Servicebio, Wuhan, China) and anti-F4/80 rabbit pAb at a 1:1000 dilution (Servicebio), overnight at 4 ℃. The following day, the sections were treated with a secondary antibody conjugated to horseradish peroxidase (HRP) and incubated for 30 min. DAB chromogenic agent was added dropwise to the tissue sections, which were then placed under a microscope for observation. The chromogenic agent was

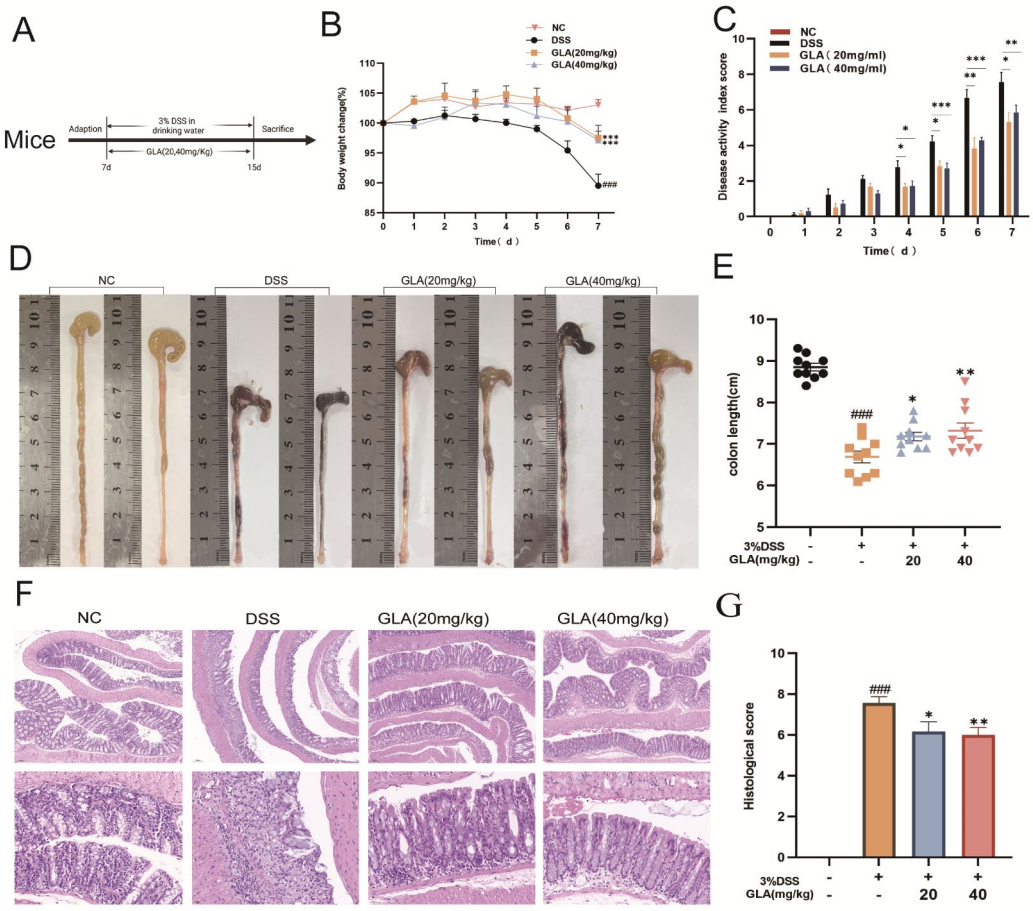

Fig. 1. Glaucocalyxin A alleviates symptoms of DSS-induced acute colitis in wild-type mice. (**A**) Design approach. (**B**) Changes in body weight of mice at 0–7 days. (**C**) Mouse DAI score. (**D**) Comparison of colon length in mice. (**E**) Statistical chart of mouse colon length. (**F**) Colon sections stained with H&E in different treatment groups. (**G**) H&E score statistics of mice. ($^{\#\#\#}p < 0.05$ relative to the NC group; $^{*}p < 0.05$, $^{**}p < 0.01$, and $^{***}p < 0.001$ relative to the DSS group) ($n = 10$ mice per group).

terminated immediately after completing the observations. Hematoxylin was used to stain the nuclei, and after dehydration, the slides were examined under a white light microscope to interpret the results. Hematoxylin staining revealed nuclei with a blue hue. A brownish-yellow color indicated the presence of a positive DAB signal. Use ImageJ software to analyze the percentage of positive area in each slide.

Measurement of the expression of inflammatory cytokines

Polymerase chain reaction (PCR) was performed to quantify the mRNA expression of inflammatory cytokines. A defined amount of TRIzol was added to the colon tissues, followed by zirconium oxide grinding beads for homogenization. After centrifugation, the supernatants were collected for RNA extraction. The reverse transcription reaction system (total volume, 20 μl) was as follows: mix 4 μl + mRNA x μl + DEPC (16 x) μl, where x is calculated as 1000 divided by the RNA concentration. GeneAmp PCR system 9700 was used for reverse transcription (37 °C for 15 min, 98 °C for 5 s, and 4 °C indefinitely). After 15 min, cDNA was obtained. A Takara kit was used to perform real-time quantitative PCR assays. Three replicates were performed for each independent experiment, and the average was calculated. Independent experiments were repeated three times. The expression levels of the target genes were normalized to those of GAPDH. Calculations were then performed using the 2^(-ΔΔCt) method. The primer sequences used for quantitative PCR were as follows: for MMGAPDH, the forward primer was AGGTCGGTGTGAACGGATTTG, and the reverse primer was GGGGTCGTTGATG GCAACA; for MMIL-6, the forward primer was CTCCCAACAGACCTGTCTATAC and reverse primer was C CATTGCACAACTCTTTTCTCA; for MMIL-1β, the forward primer was CACTACAGGCTCCGAGATGAA CAAC and reverse primer was TGTCGTTGCTTGGTTCTCCTTGTAC; for MMTNF-α, the forward primer was ATGTCTCAGCCTCTTCTCATTC and reverse primer was GCTTGTCACTCGAATTTTGAGA; and for MMIL-10, the forward primer was TTCTTTCAAACAAAGGACCAGC and reverse primer was GCAACCCA AGTAACCCTTAAAG.

Network pharmacology analysis

The relevant targets of GLA in the PharmMapper(http://www.lilab-ecust.cn/pharmmapper/) and UniProt (https://www.uniprot.org/) databases were predicted, all targets were filtered with a probability > 0, and the predicted targets of the compound were obtained. We searched the GeneCards (https://www.genecards.org/) data and OMIM (https://www.omim.org/) database using "Inflammatory Bowel Disease" as the keyword, filtered all targets with a score greater than the median, and obtained target genes for IBD. The target genes for IBD were compared with the predicted targets of GLA, and intersecting genes were considered the potential target genes associated with the effects of GLA on IBD. The STRING (https://cn.string-db.org/) database was used to calculate and output interaction information for multiple proteins. The core targets of GLA in the treatment of IBD were screened and imported into Cytoscape (version 3.10.0) software for mapping and analysis. The DAVID (https://davidbioinformatics.nih.gov/) platform was utilized to perform Gene Ontology annotations for biological functions and KEGG pathway enrichment analyses on the overlapping core targets. This process enabled the identification of key biological processes and signaling pathways through which GLA exerts its pharmacological effects. The resulting data were subsequently visualized to enhance the interpretation. Core targets were selected for molecular docking validation. PyMOL (version 2.5.2), Maestro (version 2022-4) and AutoDock (version 4.2.6) software were employed for protein and compound visualization, molecular preprocessing, and docking simulations, respectively.

Cell cultivation and processing

RAW264.7 cells were grown in DMEM supplemented with 10% fetal bovine serum. The cells were seeded in 6-well plates and allowed to adhere overnight. Subsequently, varying concentrations of GLA (0, 1, 2.5, 5, and 10 μM) were added, followed by the addition of LPS (1 μg/mL) after 2 h. The cells were then cultured for 22 h.

CCK-8 assay

RAW264.7 macrophages were prepared at a density of 5×10^4 cells/ml. A 96-well plate was placed in a cell culture incubator and incubated overnight to allow the cells to adhere. Subsequently, different concentrations of GLA solution (0, 1, 2.5, 5, 10, and 20 μM) were added to each well and co-cultured with the cells for 24 h. Upon completion of the culture, phosphate-buffered saline was added to wash each well, and a mixed medium containing 10% CCK-8 was used to replace the original culture medium. Following 2.5 h of incubation at 37 °C, the optical density was recorded at a wavelength of 450 nm.

Western blotting analysis

Network pharmacology analysis revealed that AKT is a common target of IBD and GLA. Western blot (WB) was then used to verify the expression levels of proteins involved in the PI3K/AKT/mTOR pathway. First, RIPA and PMSF were mixed at a ratio of 100:1, and the mixture was then added to the six-well plates to fully lyse the cells. A BCA protein quantification kit was used to determine the protein concentration. Appropriate amounts of loading buffer were added to each group as required. The samples were heated in a metal bath for 10 min and then stored in a -20 °C freezer. Electrophoresis buffer was prepared by mixing Tris (3.03 g), glycine (18.7 g), SDS (1 g), and H2O (1 L). Transfer buffer was prepared by combining Tris (3.03 g), glycine (14.4 g), methanol (200 ml), and H2O (800 ml). Briefly, protein samples were vortexed and centrifuged, and the supernatant was collected and loaded onto a precast gel (Tris-Gly, 4–20%) for electrophoresis at 80 mV. The position of bromophenol blue was observed using the marker. Electrophoresis was terminated when target proteins were adequately separated. A 0.22 μm PVDF membrane was activated with anhydrous methanol for 4 min, and the precast gel was transferred onto filter paper. The transfer clamp was closed, and membrane transfer. The membrane was blocked with a rapid blocking solution for 20 min. After thoroughly washing the membrane, dilutions of primary antibodies against AKT, p-AKT, PI3K, p-PI3K, mTOR and p-mTOR were prepared. The membranes were incubated overnight and thoroughly washed, and the corresponding secondary antibody was added for incubation. Finally, an ECL hypersensitive luminescence solution was prepared to detect protein expression levels.

Equipment and settings

Western blot images were acquired using a Tanon 5200 Multi Chemiluminescent Imaging System (Tanon Science & Technology) under automatic exposure mode (16-bit dynamic range), with raw data exported as 8-bit grayscale files. Image analysis was performed using ImageJ (version 1.54 g, National Institutes of Health, USA) with standardized protocols. All target protein signals were normalized to corresponding GAPDH internal controls from the same blot. Brightness/contrast adjustments, when applied, were implemented globally using linear scaling with identical parameters across experimental and control groups. No selective editing tools or non-linear manipulations were employed. Full uncropped blots, including molecular weight markers (Prestained Protein Marker II ,10–200 kDa) and membrane edges, are provided in Supplementary Information-Western Blot Repeats to verify image integrity.

Human peripheral blood mononuclear cells

Three patients with active UC were selected. After signing an informed consent form, 10 mL of whole blood was drawn and processed immediately. The plasma fraction was then removed by centrifugation. Whole blood was diluted with approximately 1 ml of normal saline with a pipette, and then the diluted blood was slowly added to a centrifuge tube containing Ficoll. After several centrifugation washes, the pellet was found to contain PBMCs. Then, 50 μl of $CD14^+$ T cell bead particles was added to every 10^7 cells and mixed well with a vortex shaker. The solution was placed immediately on a magnetic bead separator and incubated. A portion of the pre-and post-sorted cells described above was resuspended in 100 μl of PBS. The experimental tube and negative control group were incubated with 20 μl CD14 antibody in the dark. The cells were then resuspended with 300 μl of BD

buffer per tube, and flow cytometry was used to detect $CD14^+$ monocyte purity after sorting. Cells obtained from $CD14^+$ monocytes were re-mixed with RPMI-1640 medium (containing 10% FBS), counted on a cell slide, and seeded in a 6-well plate. The experimental group received 10 μM GLA treatment for a period of 24 h before being incubated. After incubation, cells from each well were harvested, and RNA was purified for subsequent RT-PCR analysis.

Statistical analysis

We used GraphPad Prism 9.5.0 software for data analysis. Prior to performing statistical tests, we assessed the normality of the data using the Shapiro-Wilk test and checked for homogeneity of variance using Levene's test. For comparisons between two groups, the t-test was employed, assuming equal variances. For comparisons involving more than two groups, we used one-way analysis of variance (ANOVA), followed by Tukey's post hoc test to adjust for multiple comparisons. Statistical significance was set at $p < 0.05$. Data are presented as the mean ± SEM.

Ethical statement

The animal experiments in this study have been approved by the Experimental Animal Center of Nantong University. All animal operations and procedures were conducted in accordance with the approved guidelines and conform to the requirements of the International Guide for the Care and Use of Laboratory Animals and the ARRIVE guidelines. Additionally, experiments involving human subjects have obtained informed consent from all participants and have been approved by the Medical Ethics Committee of the Third People's Hospital of Nantong City, with the ethics reference number EK2023092. All experiments were performed in accordance with the relevant guidelines and regulations.

Results

GLA alleviates the clinical manifestations of acute UC in mice

GLA significantly ameliorates acute UC in mice. In this study, mice with UC induced by 3% DSS showed obvious symptoms, such as diarrhea, hematochezia, unformed stool, and weight loss. Following treatment with varying doses of GLA, the mice exhibited significantly less weight loss than the model group (Fig. 1B). Beginning on the fourth day, we observed more pronounced symptoms in the DSS group. The mice exhibited loose and bloody stools, reduced activity, and dull fur. The weight, stool viscosity, and fecal occult blood of the mice were recorded daily. The DAI scores were calculated daily. Starting on the fourth day, the DAI score of the GLA-treated group was noticeably lower than that of the DSS group (Fig. 1C).

After the treatments were completed, the mice fasted for 12 h. On the 8th day, all mice were sacrificed, and the colon was isolated. Macroscopic examination of the colons of mice in each group revealed that the colon length was significantly shortened, and the colon length of GLA-treated mice was longer than that of the DSS group (Fig. 1D&E). To assess colonic histological lesions in mice, hematoxylin and eosin (H&E) staining was performed. As shown in Fig. 1F and G, inflammatory infiltration, goblet cell loss, and crypt structural changes occurred in the mucosal and submucosal layers of the colons of mice in the DSS group. Following treatment with varying doses of GLA, the inflammatory responses in the mouse colon tissue improved. The 40 mg/kg GLA-treated group exhibited a significant reduction in inflammatory cell infiltration compared to the DSS group.

GLA mitigates the DSS-induced upregulation of inflammatory factors in the colon

Myeloperoxidase (MPO) is a functional and activation marker of neutrophils, and its expression levels indicate the severity of colon inflammation. F4/80 is a marker of mouse macrophages, and its expression is significantly increased during macrophage activation. We performed MPO and F4/80 immunohistochemical staining of colon tissues in each group. In comparison with the model group, UC mice that received the GLA treatment (20 and 40 mg/kg) exhibited reduced positive expression of MPO and F4/80 (Fig. 2A–D). To assess the level of inflammation in mouse colon, PCR analysis revealed that the mRNA expression of inflammatory markers IL-6, IL-1β, and TNF-α was significantly reduced in the GLA treatment group (Fig. 2E-G), while the mRNA expression of IL-10 increased (Fig. 2H). This reduction was significant compared with that in the DSS group. This suggests that GLA effectively suppressed the DSS-induced upregulation of inflammation-related factors.

Network pharmacology suggests that GLA alleviates UC via the PI3K/AKT pathway

To clarify the mechanism of action, we performed network pharmacology analysis to identify potential targets of GLA in the treatment of IBD. Using a Venn diagram, we found that GLA and IBD had 188 common targets (Fig. 3A). The protein-protein interaction (PPI) network diagram illustrates the complex interaction between targets (Fig. 3B&C). A darker color of the target represents a higher degree value, signifying that the target plays a more prominent role in the effectiveness of GLA in treating IBD. Akt has been shown to represent one of the most relevant target genes. Previous studies have demonstrated that AKT has a significant effect on the inflammatory response in the intestines of mice[9,22]. This suggests that GLA-induced alleviation of intestinal inflammation may be related to AKT. Additionally, we constructed a disease-component-target-pathway network and performed KEGG enrichment assays (Fig. 3D–F). The findings revealed that the three most prominent signaling pathways were the PI3K/AKT, MAPK, and Ras signaling pathways (Fig. 3F). The potential mechanism by which GLA alleviates UC involves the regulation of PI3K/AKT signaling, which is essential for regulating inflammation. The molecular docking visualization results revealed that the binding energy of GLA to the AKT protein was − 6.77 $kCal \cdot mol^{[-1}$. Thus, it showed good binding activity and could be combined under natural conditions (Fig. 3G&H).

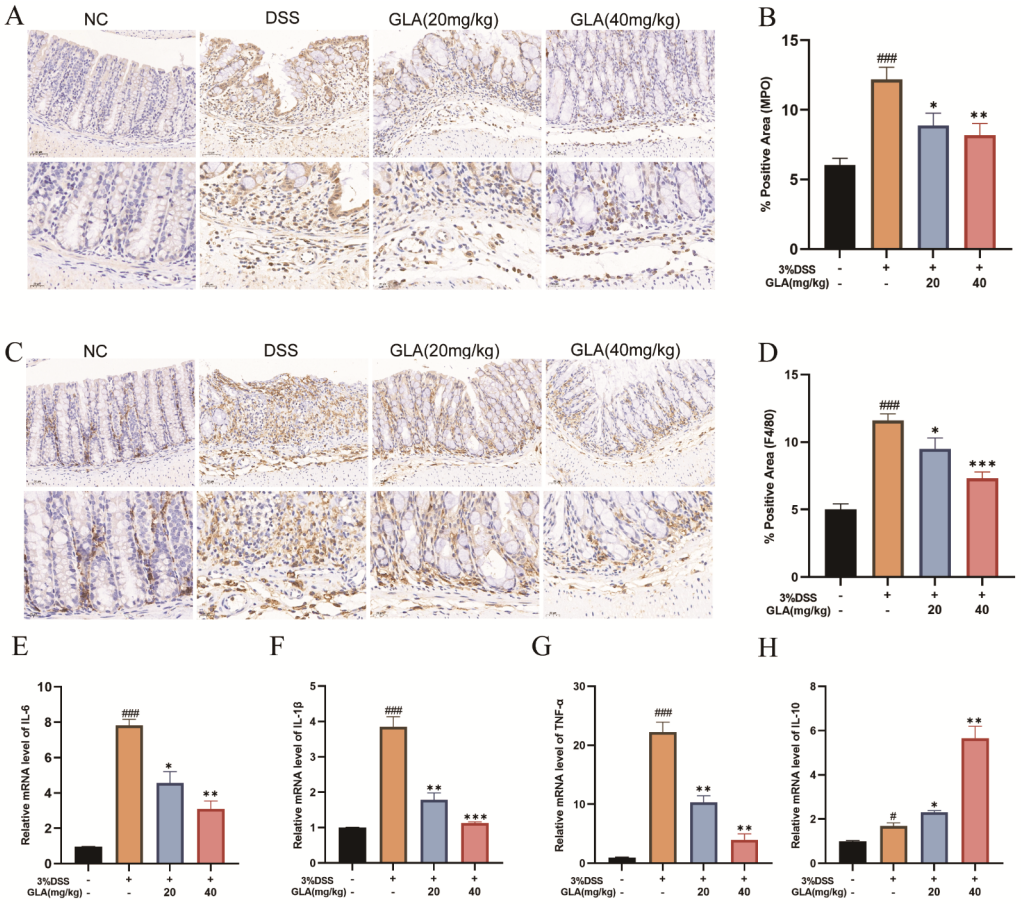

Fig. 2. The effects of GLA on inflammatory cells in colitis in mice. (**A**) MPO immunohistochemical staining of different groups. (**B**) Comparison of the percentage of %positive area (MPO) between groups, indicating high and low neutrophil expression (*$p < 0.05$ and **$p < 0.01$ relative to the control). (**C**) Immunohistochemical staining of F4/80 in different groups. (**D**) Comparison of the percentage of %positive area (F4/80) between groups, indicating high and low macrophage expression. (E&H) Concentrations of inflammatory cytokines IL-6, IL-1β, TNF-α, and IL-10 in the colonic tissues of different groups. ($^{###}p < 0.05$ and $^{##}p < 0.01$ relative to the NC group; *$p < 0.05$; **$p < 0.01$, and ***$p < 0.001$ relative to the DSS group).

GLA reduces the expression of inflammatory components in cells

Using the CCK-8 assay, we evaluated the effects of various GLA concentrations on the viability of RAW264.7 cells. The results showed that except for the 20 μM concentration, significant differences in cell survival rates were not observed relative to that of the control group. Consequently, we used the concentration gradient from this experiment in subsequent experiments (Fig. 4B). In the RAW264.7 cell model stimulated by LPS, we found that GLA markedly downregulated the mRNA of the pro-inflammatory cytokines IL-6, IL-1β, and TNF-α (Fig. 4C–F). This indicates that GLA might exert anti-inflammatory properties by suppressing the release of pro-inflammatory factors generated by macrophages.

GLA inhibits the phosphorylation of PI3K/AKT/mTOR

Based on the results from network pharmacology, Western blot analysis was performed to evaluate the expression levels of proteins related to the PI3K/ AKT pathway and its downstream effector mTOR. Total mTOR, PI3K, AKT protein levels remained stable, indicating that pathway activation is driven by post-translational modifications.The protein expression levels of p-AKT/AKT, p-PI3K/PI3K and p-mTOR/mTOR in the LPS-treated group increased significantly, indicating that LPS activated the PI3K/AKT/mTOR signaling pathway. The protein expression levels of p-AKT/AKT, p-PI3K/PI3K and p-mTOR/mTOR in the GLA-treated groups decreased significantly, indicating that GLA can effectively inhibit LPS-induced phosphorylation of AKT at Ser473, PI3K at the p85 Tyr458 site and mTOR at Ser2448. This finding suggests its role in suppressing PI3K/AKT/mTOR signaling and alleviating the inflammatory response (Fig. 5).

GLA suppresses the production of inflammatory cytokines in active UC patients

Using magnetic bead sorting, we isolated peripheral blood mononuclear cells with high purity from patients with UC (Supplementary Information). Following co-culture with GLA, the mRNA levels of IL-6, TNF-α, and IL-1β in monocytes were significantly reduced. In contrast, the mRNA levels of the anti-inflammatory cytokine IL-10

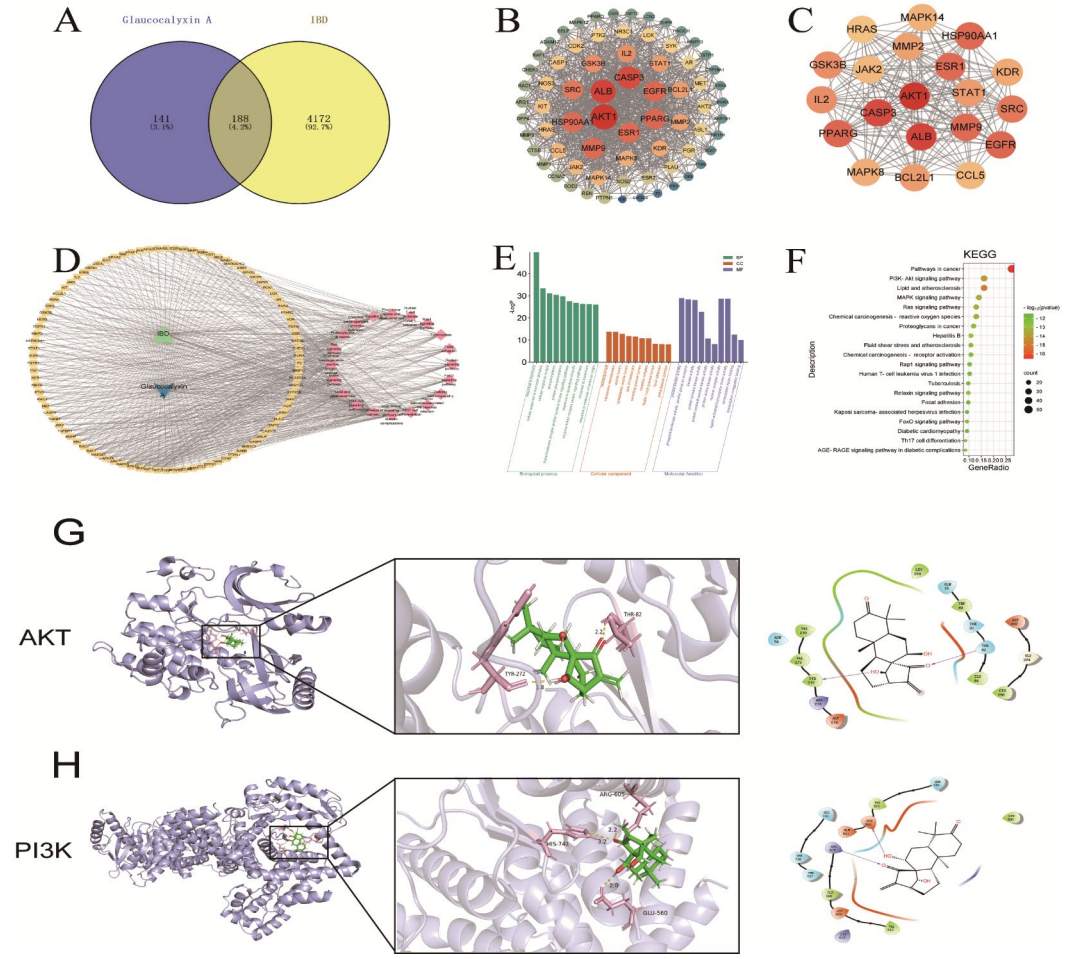

Fig. 3. Identification of candidate targets for GLA against IBD. (**A**) Venn plot showing the intersection of GLA and IBD-related genes. (**B**) Protein-protein interaction (PPI) networks. The nodes represent proteins, and the edges represent the interactions between proteins. The size and shade of color of a node are directly proportional to its connectivity, with nodes with higher connectivity appearing larger and darker in color. (**C**) Sub-networks of important hub genes in the PPI network. These central hub genes may play an important role in the pathophysiology of IBD. (**D**) Gene-disease association networks. The yellow triangles represent the common targets, and the pink nodes represent the signaling pathways associated with them. (**E**) Functional enrichment analysis of common targets. (**F**) KEGG pathway enrichment analysis. The bubble map shows the significantly enriched pathways, and the size and color of the bubbles indicate the number of enriched genes and significance of the difference, respectively, thus revealing the underlying biological pathways. Docking conformation of GLA to key target proteins. (**G**) GLA with AKT. (**H**) GLA with PI3K.

increased markedly (Fig. 6A–D). These findings suggest that GLA can significantly alleviate the inflammatory state in active UC.

Discussion

Recurrent intestinal inflammation has detrimental effects on the physical and mental health of patients with UC. UC may not cause irreversible damage, such as Crohn disease (CD), although it is still a serious disease[23]. Although current clinical treatments have led to cases of remission, biologics are expensive, and treatment is often ineffective or leads to serious side effects[24–26]. Therefore, there is an urgent need to identify medications with fewer side effects, better quality, and lower costs. In recent years, researchers have begun to study how different traditional Chinese medicine compounds alleviate UC. Their aim was to identify alternative treatments that are affordable and have fewer adverse effects. Research revealed that a compound derived from Chinese yam significantly reduces the production of inflammatory cytokines associated with UC, suppresses the activation of inflammatory signaling pathways, and promotes the restoration of tight junction protein expression in the intestinal lining[27]. Berberine can inhibit the excessive activation of macrophages to modulate immune responses, and it regulates the composition and function of the intestinal microbiota and enhances the functionality of the intestinal barrier[28,29]. These multiple mechanisms indicate that berberine may represent a viable and promising option for the treatment of UC. Rhein helps alleviate intestinal inflammation in UC by acting on the gut microbiota and lowering uric acid levels[30]. Although the aforementioned traditional Chinese

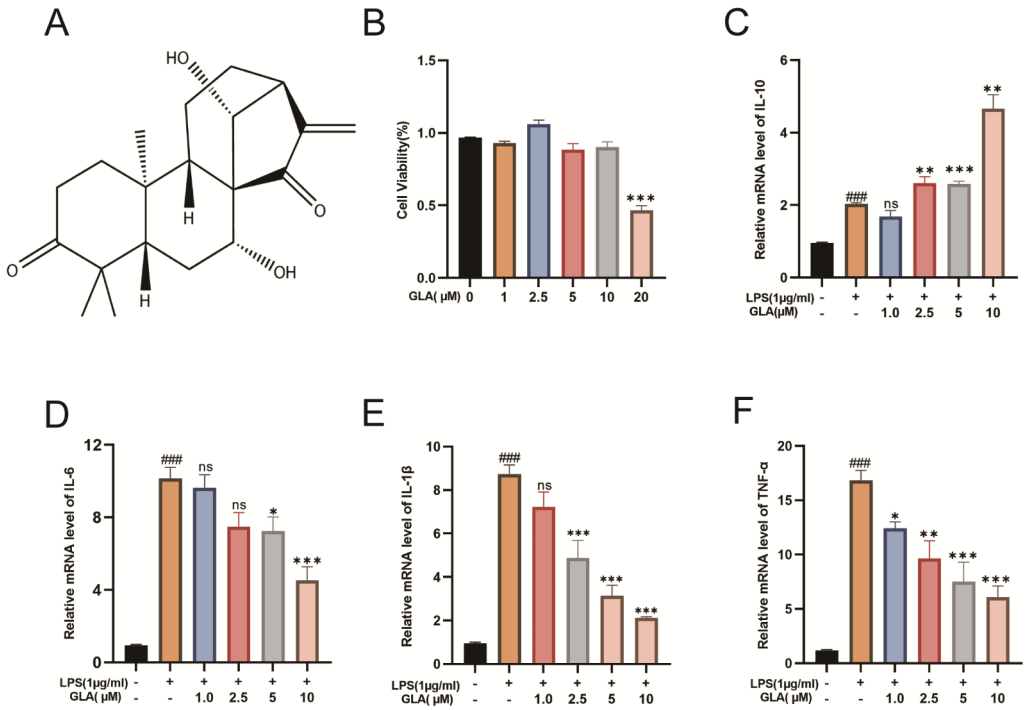

Fig. 4. GLA suppresses the LPS-induced increase in the expression of inflammatory components in a macrophage model of inflammation in RAW264.7 cells. (**A**) Chemical Structure of Glaucocalyxin A. (**B**) Assessment of the Cytotoxicity of Different GLA Concentrations on Raw264.7 Cells. (**C**) With increasing GLA concentration, IL-10 expression increases. (**D**) With increasing GLA concentration, IL-6 expression decreases. (**E**) With increasing GLA concentration, IL-1β, expression decreases. (**F**) With increasing GLA concentration, TNF-α expression decreases. (*$p < 0.05$; **$p < 0.01$; and ***$p < 0.001$ relative to the control).

medicine monomers may have the potential to alleviate UC, the mechanisms of many other components remain inadequately understood. These unexplored components may act through various pathways, including inhibition of inflammation, regulation of immune function, and protection of the intestinal barrier. Therefore, additional studies are required to thoroughly investigate the mechanisms underlying the effects of these traditional Chinese medicine constituents, determine their specific roles in the treatment of UC, and identify the optimal methods for their use.

GLA was first isolated in 1981. Since then, it has been found to exhibit inflammation-modulating, reactive oxygen species (ROS)-neutralizing, antitumor and immunoregulatory effects. GLA inhibits the advancement of osteoarthritis (OA) in both in vivo and in vitro models by blocking the activation of the NF-κB and MAPK pathways and significantly downregulating the expression of IL-1β and PGE2[31]. GLA reduces the concentration of inflammatory mediators in CCl_4-induced liver fibrosis and helps restore the balance of the gut microbiota[32]. GLA also limits multiple myeloma cell proliferation by targeting and repressing STAT3 expression, which helps slow the progression of multiple myeloma[17]. GLA is a broadly applicable natural active formula with great potential for applications in anti-inflammatory, antitumor, and immunoregulatory therapies. Because of its broad functionality, this compound is a promising candidate for application in various fields. However, the potential benefits and underlying mechanisms of GLA in the treatment of IBD have not yet been investigated. Thus, further research is required to thoroughly explore its roles in treating IBD. This is the first study to explore the ability of GLA to alleviate colonic inflammation. Acute UC was induced in mice using 3% DSS, and intraperitoneal injections of GLA at 20 and 40 mg/kg were administered to the treatment groups daily. The results revealed that GLA alleviated symptoms such as shortened colon length, loose stools, and weight loss in mice. Histopathological analysis showed that GLA suppressed colonic and glandular structure damage, crypt loss, and inflammatory cell infiltration. Thus, our findings revealed that GLA effectively alleviated acute UC in mice. Furthermore, our results indicate that the histological scores in the GLA 40 mg/kg group were improved compared to those in the 20 mg/kg group; however, the clinical DAI scores on days 6–7 showed the opposite trend, possibly due to the optimal therapeutic concentration of GLA. Next, we will further investigate the maximum safe dose of GLA for treating UC.

To further investigate the mechanism by which GLA alleviates colonic inflammation, we performed immunohistochemical staining, which revealed that GLA treatment diminished the expression of MPO and F4/80 in mouse colonic tissues. F4/80 is a specific glycoprotein marker that is widely present in tissue-resident macrophages in mice, and it is commonly used to study the distribution and function of macrophages[33]. The higher its positive expression, the more severe the intestinal inflammation. Excessive macrophage activation is a key feature of IBD[34]. Macrophages in the intestine are highly adaptable and can differentiate into two polarized

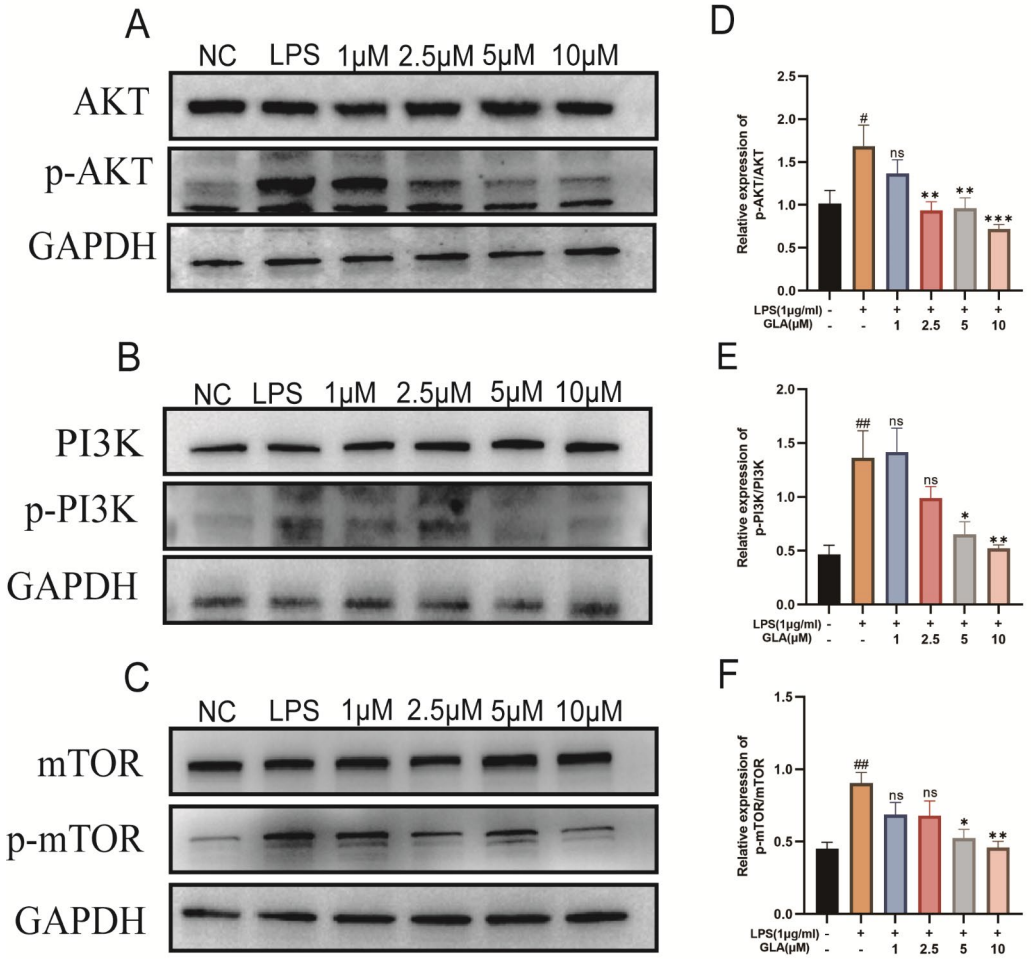

Fig. 5. GLA inhibits the PI3K/AKT/mTOR signaling pathway. (**A**&**B**&**C**) In the LPS-induced RAW264.7 cell inflammation model, cells were co-cultured with varying concentrations of GLA for 24 h. (**D**&**E**&**F**) Protein levels were quantified using ImageJ. The full-length uncropped blots are presented in the Supplementary Information - Western Blot Repeats section. (##$p < 0.01$ relative to the NC group, *$p < 0.05$ and **$p < 0.01$ relative to the LPS group).

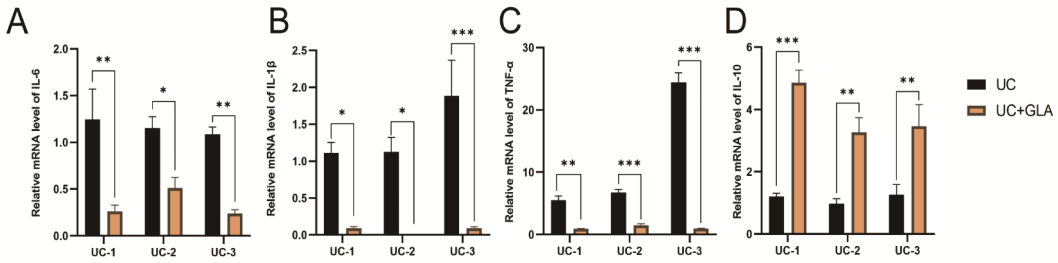

Fig. 6. Effect of GLA on peripheral blood mononuclear cells in patients with active UC. (**A**&**B**&**C**) GLA effectively inhibited the expression of IL-6, IL-1β, and TNF-α. (**D**) GLA promoted the expression of IL-10. (*$p < 0.05$, **$p < 0.01$, and ***$p < 0.001$).

states depending on environmental changes[35]. When intestinal inflammation occurs, macrophages tend to secrete pro-inflammatory cytokines such as IL-6, IL-1β, and TNF-α, thereby exacerbating the inflammation. Simultaneously, some macrophages release inhibitory cytokines such as IL-10 to help alleviate inflammation[36,37]. The GLA-induced alleviation of UC may be related to the modulation of macrophage function by GLA, as evidenced by the expression levels of inflammatory cytokines in the colonic tissues of the mice. To further explore the mechanism underlying the anti-colitis effects of GLA, we conducted a network pharmacology analysis. The

key shared target between GLA and inflammatory bowel disease is AKT. mTOR is an important downstream protein of the PI3K/AKT pathway closely related to an overreaction of immune cells in many autoimmune diseases[38]. Our experimental findings suggest GLA's anti-inflammatory activity may involve modulation of the PI3K/AKT/mTOR pathway. Previous studies have shown that GLA can alleviate RANKL-induced inflammation in RAW264.7 cells by inhibiting the activation of AKT. This suggests the potential mechanism underlying its anti-inflammatory effects[39]. AKT acts as a primary effector of PI3K and is a vital component of the PI3K/AKT signaling cascade, which is crucial for regulating cellular growth, proliferation, and metabolism[40]. In acute UC in mice, the AKT signaling pathway can activate macrophages, thereby influencing both the intensity and duration of the inflammatory response. The abnormal activation of the AKT/PI3K pathway in macrophages results in excessive intestinal inflammation and tissue damage[41,42]. Therefore, we established an LPS-induced inflammation model using macrophages. LPS induces the expression of the pro-inflammatory cytokines TNF-α, IL-1β, and IL-6 by activating downstream signaling pathways by binding to TLR4 on the surface of macrophages. In this study, PCR was used to assess the mRNA expression of various inflammatory factors in the cellular models. The results demonstrated that the expression of these inflammatory factors significantly decreased in the groups treated with different concentrations of GLA, which was attributed to the regulation of the AKT pathway. This decrease may be attributed to the GLA-mediated inhibition of AKT signaling, which weakened the transmission of inflammatory signals. Inhibition of AKT signaling may further suppress the activation of downstream transcription factors such as NF-κB, thereby leading to a decrease in the transcription levels of pro-inflammatory cytokine genes. Western blot analysis revealed that the proteins associated with the PI3K/AKT signaling pathway were upregulated in LPS-treated RAW264.7 cells, which was significantly reversed upon GLA treatment. Our findings suggest that GLA may regulate macrophage function by inhibiting PI3K/AKT/mTOR signaling, thereby reducing the mRNA expression of the inflammatory cytokines IL-6, IL-1β, and TNF-α.

Studies have shown that macrophages derived from monocyte differentiation are more abundant in the intestine[33]. Therefore, we selected peripheral blood samples from patients with active UC to extract high-purity monocytes (> 95% purity). In this study, treatment with GLA (10 μM) significantly reduced the IL-6 and IL-1β levels in monocytes from UC patients but notably increased the IL-10 levels. Through animal experiments, cell studies, network pharmacology, and human peripheral blood analysis, we collectively confirmed that GLA can alleviate IBD symptoms by inhibiting macrophage activation via the PI3K/AKT/mTOR signaling pathway. In addition, GLA is inexpensive and readily available, thus offering a new approach to the clinical treatment of patients with IBD.

However, to date, no studies have directly compared GLA with the current commonly used UC therapeutics in clinical practice. To better assess the relative efficacy of GLA, future studies will need to systematically compare it with these standard treatment regimens. Owing to GLA's low polarity, poor water solubility, rapid elimination from the body, short half-life, and low bioavailability, it cannot be directly used as a drug in clinical settings. Currently, numerous studies have adopted nanocarriers to encapsulate traditional Chinese medicine monomers as a solution to such issues. Genistein (GEN) has shown potential in preventing and alleviating colitis[43],however, its clinical application is significantly limited by its low water solubility and bioavailability. Previous studies have demonstrated that the use of nanocarriers (GEN-NP2) can enhance its bioavailability while maintaining its chemical stability and enabling controlled release at the site of pathology[44]. Berberine (BBR) also exhibits protective and alleviative effects against colonic inflammation[29,45]. Due to its low bioavailability in vivo, researchers have synthesized BBR-loaded carboxymethyl chitosan nanoparticles, which have demonstrated targeted therapeutic efficacy in ameliorating murine colitis[46]. These nano-drug delivery systems have significantly enhanced bioavailability. Previous studies have demonstrated that GLA-loaded nanoparticles exhibit superior anti-tumor activity both in vitro and in vivo[47]. Building on these evidences, we are actively developing advanced delivery strategies, including nanoparticle encapsulation or prodrug modification, to optimize GLA's pharmacokinetic profile for IBD treatment. More suitable delivery methods need to be explored, and considerable work must be performed before this therapeutic strategy can be applied in clinical practice.

Conclusion

Our previous research revealed that GLA can alleviate UC by reducing the levels of inflammatory cytokines. Thus, in the present study, we investigated a mouse inflammation model, RAW264.7 cell model, and human peripheral blood samples and found that GLA reduced the mRNA expression of pro-inflammatory cytokines while increasing the mRNA expression of anti-inflammatory cytokines. GLA also reduced the expression of MPO and F4/80 in colon tissues and inhibited LPS-induced phosphorylation and activation of the PI3K/AKT/mTOR pathways. Therefore, GLA has significant potential as a therapeutic agent for treating IBD and may offer new treatment options for autoimmune diseases.

Data availability

All the data are reliable, and all the reagents and devices designed in the article are commercially available. Please contact the corresponding author for the data if required.

Received: 29 November 2024; Accepted: 19 February 2025
Published online: 24 February 2025

References

1. Agrawal, M., Allin, K. H., Petralia, F., Colombel, J. F. & Jess, T. Multiomics to elucidate inflammatory bowel disease risk factors and pathways. *Nat. Rev. Gastroenterol. Hepatol.* https://doi.org/10.1038/s41575-022-00593-y (2022).
2. Kaplan, G. G. & Windsor, J. W. The four epidemiological stages in the global evolution of inflammatory bowel disease. *Nat. Rev. Gastroenterol. Hepatol.* **18**, 56–66 (2020).

3. Almradi, A. et al. Clinical trials of IL-12/IL-23 inhibitors in inflammatory bowel disease. *BioDrugs* **34**, 713–721 (2020).
4. Berends, S. E., Strik, A. S., Löwenberg, M., D'Haens, G. R. & Mathôt, R. A. A. Clinical Pharmacokinetic and pharmacodynamic considerations in the treatment of ulcerative colitis. *Clin. Pharmacokinet.* **58**, 15–37 (2018).
5. Saez, A., Herrero-Fernandez, B., Gomez-Bris, R., Sánchez-Martinez, H. & Gonzalez-Granado, J. M. Pathophysiology of inflammatory bowel disease: Innate Immune system. *IJMS* **24**, 1526 (2023).
6. Na, Y. R., Stakenborg, M., Seok, S. H. & Matteoli, G. Macrophages in intestinal inflammation and resolution: A potential therapeutic target in IBD. *Nat. Rev. Gastroenterol. Hepatol.* **16**, 531–543 (2019).
7. Hegarty, L. M., Jones, G. R. & Bain, C. C. Macrophages in intestinal homeostasis and inflammatory bowel disease. *Nat. Rev. Gastroenterol. Hepatol.* https://doi.org/10.1038/s41575-023-00769-0 (2023).
8. Jones, G. R. et al. Dynamics of Colon monocyte and macrophage activation during colitis. *Front. Immunol.* **9**, (2018).
9. Li, N. et al. Stimulation by exosomes from hypoxia-preconditioned hair follicle mesenchymal stem cells facilitates mitophagy by inhibiting the PI3K/AKT/mTOR signaling pathway to alleviate ulcerative colitis. *Theranostics* **14**, 4278–4296 (2024).
10. Dong, Y. et al. Targeting CCL2-CCR2 signaling pathway alleviates macrophage dysfunction in COPD via PI3K-AKT axis. *Cell. Commun. Signal.* **22**, (2024).
11. Afzal, O. et al. mTOR as a potential target for the treatment of microbial infections, inflammatory bowel diseases, and colorectal Cancer. *IJMS* **23**, 12470 (2022).
12. Zhang, T., Zhao, L., Xu, M., Jiang, P. & Zhang, K. Moringin alleviates DSS-induced ulcerative colitis in mice by regulating Nrf2/NF-κB pathway and PI3K/AKT/mTOR pathway. *Int. Immunopharmacol.* **134**, 112241 (2024).
13. Li, M. et al. Huangqin Decoction ameliorates DSS-induced ulcerative colitis: Role of gut microbiota and amino acid metabolism, mTOR pathway and intestinal epithelial barrier. *Phytomedicine* **100**, 154052–154052 (2022).
14. Dong, L. et al. Anti-inflammatory effect of Rhein on ulcerative colitis viainhibiting <scp>PI3K</scp>/Akt/<scp>mTOR</scp> signaling pathwayand regulating gut microbiota. *Phytother. Res.* **36**, 2081–2094 (2022).
15. Zhu, H. et al. Triptolide attenuates LPS-induced activation of RAW 264.7 macrophages by inducing M1-to-M2 repolarization via the mTOR/STAT3 signaling. *Immunopharmacol. Immunotoxicol* **44**, 894–901 (2022).
16. Wang, M., Xu, B., Liu, L. & Wang, D. Oridonin attenuates dextran sulfate sodiuminduced ulcerative colitis in mice via the Sirt1/NFκB/p53 pathway. *Mol. Med. Rep.* **26**, (2022).
17. Li, M. et al. Glaucocalyxin A suppresses multiple myeloma progression in vitro and in vivo through inhibiting the activation of STAT3 signaling pathway. *Cancer Cell. Int.* **21**, (2021).
18. Lin, W. et al. Glaucocalyxin A induces G2/M cell cycle arrest and apoptosis through the PI3K/Akt pathway in human bladder cancer cells. *Int. J. Biol. Sci.* **14**, 418–426 (2018).
19. Hou, X. et al. Glaucocalyxin A alleviates LPS-mediated septic shock and inflammation via inhibiting NLRP3 inflammasome activation. *Int. Immunopharmacol.* **81**, 106271 (2020).
20. Zhu, W., Zhang, Y., Li, Y., Wu, H. & Glaucocalyxin A attenuates IL-1β-Induced inflammatory response and cartilage degradation in osteoarthritis chondrocytes via inhibiting the activation of NF-κB signaling pathway. *Dis. Markers* 1–9 (2022). (2022).
21. Wen, X. D. et al. Panax notoginsengattenuates experimental colitis in the azoxymethane/dextran sulfate sodium mouse model. *Phytother Res.* **28**, 892–898 (2013).
22. Schwanke, R. C. et al. Oral administration of the flavonoid myricitrin prevents dextran sulfate sodium-induced experimental colitis in mice through modulation of PI3K/Akt signaling pathway. *Mol. Nutr. Food Res.* **57**, 1938–1949 (2013).
23. Le Berre, C., Ananthakrishnan, A. N., Danese, S., Singh, S. & Peyrin-Biroulet, L. Ulcerative colitis and Crohn's disease have similar burden and goals for treatment. *Clin. Gastroenterol. Hepatol.* **18**, 14–23 (2020).
24. Na, S. Y. & Moon, W. Perspectives on current and novel treatments for inflammatory bowel disease. *Gut Liver* **13**, 604–616 (2019).
25. Chan, H. C. & Ng, S. C. Emerging biologics in inflammatory bowel disease. *J. Gastroenterol.* **52**, 141–150 (2016).
26. Yang, L. et al. A recent update on the use of Chinese medicine in the treatment of inflammatory bowel disease. *Phytomedicine* **92**, 153709 (2021).
27. Li, P. et al. Structural characteristics of a Mannoglucan isolated from Chinese Yam and its treatment effects against gut microbiota dysbiosis and DSS-induced colitis in mice. *Carbohydr. Polym.* **250**, 116958 (2020).
28. Takahara, M. et al. Berberine improved experimental chronic colitis by regulating interferon-γ- and IL-17A-producing lamina propria CD4 + T cells through AMPK activation. *Sci. Rep.* **9**, (2019).
29. Zhu, L., Gu, P. & Shen, H. Protective effects of Berberine hydrochloride on DSS-induced ulcerative colitis in rats. *Int. Immunopharmacol.* **68**, 242–251 (2019).
30. Wu, J. et al. Rhein modulates host purine metabolism in intestine through gut microbiota and ameliorates experimental colitis. *Theranostics* **10**, 10665–10679 (2020).
31. Hong, X. et al. Glaucocalyxin A delays the progression of OA by inhibiting NF-κB and MAPK signaling pathways. *J. Orthop. Surg. Res.* **19**, (2024).
32. Qu, R. et al. Glaucocalyxin A attenuates carbon < scp > tetrachloride-induced liver fibrosis and improves the associated gut microbiota imbalance. *Chem. Biol. Drug Des.* **102**, 51–64 (2023).
33. Bain, C. C., Schridde, A. & Origin Differentiation, and function of intestinal macrophages. *Front. Immunol.* **9**, (2018).
34. Martin, J. C. et al. Single-Cell analysis of Crohn's disease lesions identifies a pathogenic cellular module associated with resistance to Anti-TNF therapy. *Cell* **178**, 1493–1508e20 (2019).
35. Mantovani, A., Allavena, P., Marchesi, F. & Garlanda, C. Macrophages as tools and targets in cancer therapy. *Nat. Rev. Drug Discov.* **21**, 799–820 (2022).
36. Chen, S. et al. Macrophages in immunoregulation and therapeutics. *Sig Transduct. Target. Ther.* **8**, (2023).
37. Han, X., Ding, S., Jiang, H. & Liu, G. Roles of macrophages in the development and treatment of gut inflammation. *Front. Cell. Dev. Biol.* **9**, (2021).
38. Zhang, L. & Wei, W. Anti-inflammatory and immunoregulatory effects of Paeoniflorin and total glucosides of Paeony. *Pharmacol. Ther.* **207**, 107452 (2019).
39. Zhu, M. et al. Glaucocalyxin A suppresses osteoclastogenesis induced by RANKL and osteoporosis induced by ovariectomy by inhibiting the NF-κB and Akt pathways. *J. Ethnopharmacol.* **276**, 114176 (2021).
40. Vanhaesebroeck, B., Stephens, L. & Hawkins, P. PI3K signalling: The path to discovery and Understanding. *Nat. Rev. Mol. Cell. Biol.* **13**, 195–203 (2012).
41. Liu, B. et al. Kuijieyuan Decoction improved intestinal barrier injury of ulcerative colitis by affecting TLR4-Dependent PI3K/AKT/NF-κB oxidative and inflammatory signaling and gut microbiota. *Front. Pharmacol.* **11**, (2020).
42. Ni, L. et al. Periplaneta americana extract ameliorates dextran sulfate sodium-induced ulcerative colitis via immunoregulatory and PI3K/AKT/NF-κB signaling pathways. *Inflammopharmacol* **30**, 907–918 (2022).
43. Sahoo, D. K. et al. Oxidative stress, hormones, and effects of natural antioxidants on intestinal inflammation in inflammatory bowel disease. *Front. Endocrinol.* **14**, (2023).
44. Fan, W. et al. Genistein-Derived ROS-Responsive nanoparticles relieve colitis by regulating mucosal homeostasis. *ACS Appl. Mater. Interfaces* **13**, 40249–40266 (2021).
45. Zhu, C. et al. Berberine a traditional Chinese drug repurposing: Its actions in inflammation-associated ulcerative colitis and cancer therapy. *Front. Immunol.* **13**, (2022).
46. Zhao, L. et al. Berberine-Loaded carboxylmethyl Chitosan nanoparticles ameliorate DSS-Induced colitis and remodel gut microbiota in mice. *Front. Pharmacol.* **12**, (2021).

47. Han, M., Li, Z., Guo, Y., Zhang, J. & Wang, X. A nanoparticulate drug-delivery system for glaucocalyxin A: Formulation, characterization, increased in vitro, and vivo antitumor activity. *Drug Deliv*. **23**, 2457–2463 (2015).

Author contributions

The study was designed by Zhaolian Bian and Tongtong Zhou. Experiments were carried out by Tongtong Zhou, with Yujing Ye, Weijie Chen, Lulu Ding, and Yanyan Wang providing experimental support. Data analysis was conducted by Leilei Luo, Jian Chen, and Lixian Wei. The manuscript was written by Tongtong Zhou and reviewed and revised by Zhaolian Bian. All authors read and approved the final manuscript.

Funding

This study was supported by grants from the Nantong Science and Technology Bureau Municipal Science and Technology Plan (JC2023115),Postgraduate Research & Practice Innovation Program of Jiangsu Province(SJCX23_1807). However, the funding sources had no involvement in the study design, collection, analysis, interpretation of data, writing of the report, or the decision to submit the paper for publication.

Declarations

Competing interests

The authors declare no competing interests.

Consent to publish

All the authors of this article have consented to publication.

Additional information

Supplementary Information The online version contains supplementary material available at https://doi.org/10.1038/s41598-025-91358-5.

Correspondence and requests for materials should be addressed to Z.B.